Tethys

Journal of Mediterranean
Meteorology & Climatology

Water vapour accumulation mechanisms in the Western Mediterranean Basin and the development of European extreme rainfalls

E. Sáez de Cámara[1], G. Gangoiti[1], L. Alonso[1], M. Navazo[1], N. Gómez[1], J. Iza[1], J. A. García[1], J. L. Ilardia[1] and M. M. Millán[2]

[1]Escuela Técnica Superior de Ingeniería de Bilbao, Euskal Herriko Unibertsitatea; C/ Alameda de Urquijo s/n, E-48013 Bilbao
[2]Fundación Centro de Estudios Ambientales del Mediterráneo; C/ Charles Darwin 14, Parque Tecnológico, Paterna, E-46980 València

Correspondence to: estibaliz.saezdecamara@ehu.es

Abstract

This paper examines the role of a recently described warm season circulation at the middle troposphere of northern Africa and that of the recirculation-accumulation mode of the Western Mediterranean Basin (WMB) in the initiation of rainfall episodes in central and eastern Europe. Both of these atmospheric mechanisms can accumulate not only soil dust and pollutants for several days but also water vapour by evaporation both over the subtropical Atlantic and the western and central Mediterranean. Accumulation layers are vented off into the surrounding area after the irruption of perturbations. In particular, this work explores the exportation of water vapour under perturbed conditions associated with the passage of 'Vb' cyclones. The exceptional rainfall experienced over large areas of central Europe (Elbe/Danube floods) during August 11-13, 2002 is exposed as a case study. The procedure to simulate the mechanisms involves a combination of the Regional Atmospheric Modelling System and HYbrid PArticle Concentration and Transport modelling systems. MODIS water vapour products, radio-soundings, wind profiler radars and surface-satellite precipitation data are used to verify the simulation outputs. Our results show that most of the precipitation occurring in the target area during the initiation and deepening of the episode was very likely originated in an air mass exported from the WMB. After our tracking experiment, that air mass, with an initial Atlantic origin, entered the WMB and circulated during 4 days (August 6-9) within the marine boundary layer and the coastal range of mountains of the WMB, accumulating vapour. Then, most of it was transported on August 10, after the irruption of the 'Vb' cyclone Ilse, through the Italian Peninsula and the Adriatic Sea, across the Western Balkans into the target area. The transported vapour together with evaporation en route initiated the rainfall episode.

1 Introduction

As put forward in the study of the long time-series of the Hohenpeissenberg Observatory in southern Germany (1881-2001) by Fricke and Kaminski (2002), the frequency of intense summer precipitations is likely to have increased in many areas of central and eastern Europe. One of the most recent severe events was the August 11-13 2002 flood, which caused 36 deaths and over 15 billion USD damage (Mudelsee et al., 2004). Flash floods started in small rivers in Austria, Bohemia and the Erz Mountains, which were followed by record-breaking and violent floods of larger rivers: the Vltava, Elbe and parts of the Danube catchment. In Zinnwald-Georgenfeld (Saxony) a precipitation of 312 mm was recorded from August 12 at 06 UTC to August 13 at 06 UTC, which is the heaviest one-day total ever observed in Germany (Ulbrich et al., 2003a).

There is concern that the occurrence of such events could increase as a result of the more frequent occurrence of weather types associated with 'Vb' tracks (Van Bebber, 1891). This atmospheric circulation pattern, characterized by a low-pressure system travelling from the Western Mediterranean Basin (WMB) north-eastwards, is related to flooding in central and eastern Europe (Mudelsee et al., 2004). In addition, the anthropogenically induced climate change has been hypothesized to play an important role in the acceleration of the hydrological cycle and the flood risk due to a warmer atmosphere. The relative importance of these potential causal mechanisms is still open to discussion (Ulbrich et al., 2003b; Mudelsee et al., 2004; Christensen and Christensen, 2003).

Another question that deserves further consideration is the identification of the main source areas of the water vapour exported to Europe during these events. An analysis of back trajectories of air masses ending in central Europe on August 11-13 2002 made by Ulbrich et al. (2003b), pointed to the WMB as the main vapour source. Similar results were obtained by James et al. (2004), but only for the initial stages of the rainfall events. Millán et al. (2005) have brought attention to a water vapour accumulation excess over the WMB in recent years due to land use changes (deforestation, urbanization, and reduction of wetlands) and increased air pollution, which could also explain the observed increase of torrential rains.

A recent theory (Millán et al., 1997; Gangoiti et al., 2001, 2006a) indicates that this basin behaves like a 'holding tank' during the warm season. From approximately late April to early October the combined up-slope winds and coastal sea breezes, their return flows aloft, and their compensatory subsidence over the sea, become self-organized in vertical and horizontal recirculations that extend to the whole WMB. Thus, in contrast with regions dominated by advection and without requiring the high evaporation rates of tropical latitudes, in the Western basin the vapour, together with pollutants, is accumulated over the sea in layers piled up to 3000-4000 m. After a few days, the passage of a perturbation can vent these large, polluted, moist and potentially unstable air masses off, feeding torrential rains when convergence and lifting mechanisms are also present or alternatively they can produce pollution episodes in other parts of the basin or even in the neighbouring regions.

A similar process occurs in northern Africa around the Atlas Mountains (Gangoiti et al., 2006a). In this case, the convergence that takes place at the N-African thermal low accumulates over the northern Africa middle troposphere the pollutants and water vapour available in the Marine Boundary Layer (MBL) located at its Atlantic and Mediterranean coastal areas as well as the soil dust that is fed by the daytime up-slope flows in the southern flanks of the Atlas Mountains. These upper reservoir layers move around these mountains following the induced circulation of the N-African anticyclone until the passage of a frontal system over the Mediterranean exports a fraction of the accumulated material into

Table 1. Mean BIAS, root mean square vector error (RMSVE), root mean square errors (RMSE) and correlation coefficients between the wind profiler radars data and the simulated u and v wind components at Bilbao and Basel.

	Bilbao	Basel
BIAS u	-1.14	1.05
BIAS v	-0.42	-1.84
RMSVE	3.47	4.88
RMSE u	2.68	3.03
RMSE v	1.66	3.20
R u	0.74	0.73
R v	0.82	0.63

Europe and another fraction back into the N-African circulation.

The effects of the massive exportation of these reservoir layers on the hydrological cycle and/or the atmospheric composition of neighbouring areas merit further study. The present study was designed to investigate what role, if any, these reservoir layers located over the WMB and northern Africa play in the heavy summer precipitation episode of central and eastern Europe during August 11-13, 2002. The paper is divided into 5 sections. The details of the synoptic scenario and methodology are described in Sections 2 and 3, correspondingly. Section 4 concentrates on the description of the sequence of events during the precipitation episode as well as on the discussion on the origin of the air masses converging over the target area. Finally, Section 5 provides a summary of the main conclusions.

2 The precipitation episode of August 11-13, 2002: synoptic scenario

The meteorological situation leading to the August 11-13, 2002 flood was marked by a low pressure system, named *Ilse* by the German Weather Service, originated near Ireland. Following the path of typical Vb-tracks, it passed over the Western Mediterranean Sea and, then, moved north-eastwards to reach Central Europe. Figure 1 shows the NCEP reanalysis mean sea level pressure and the prevailing winds on August 6, 9, 12 and 15. The first panel (August 6) shows the typical synoptic pattern during the warm season of the Mediterranean: relative high pressures over the western basin and sea-breeze convergence over the mountain slopes of eastern Iberia and northern Africa. A further discussion on the summer climatology of the region can be found in Gangoiti et al. (2006a). The weak low pressure, which formed between the Gulf of Genoa and the Alps during night time from August 5 to 6 and left important rainfalls at central Europe on August 6-7, is observed out of the WMB: over the Adriatic Sea moving eastward across the Western Balkans. Figure 1b, shows the situation preceding the irruption of the Atlantic cyclone *Ilse* into the WMB.
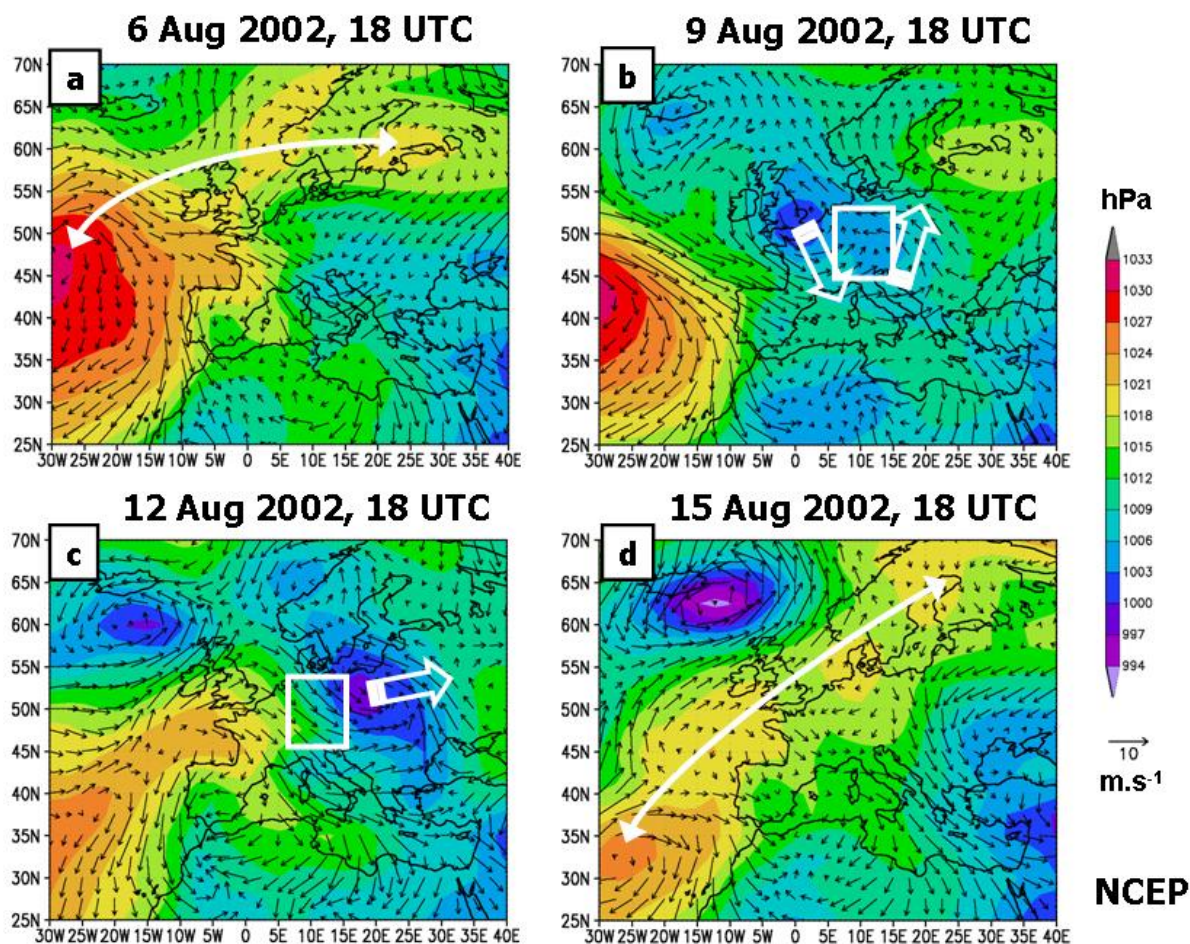
Figure 1. Evolution of mean sea level pressure and wind fields from August 6 to August 15. (a) Normal conditions over the Western Mediterranean and Northern Africa, (b) just before the irruption of cyclone *Ilse* into the Western Mediterranean basin, (c) when leaving the area, moving to the NE and (d) the re-establishment of normal conditions. Thin arrows (panels a and d) illustrate the ridge of high pressures extending from Azores into the Baltic Sea that prevents the incursion of Atlantic depressions and their frontal systems into the Western Mediterranean basin. The white open arrows show trajectories of the cyclone around the target area, which is marked by a white square. Source: NCEP Reanalysis-2 data set.

Normal conditions, prevailing over the region from August 6 to 9, favour the accumulation of pollutants as shown by Millán et al. (1992, 1996, 1997) and Gangoiti et al. (2001, 2006a) and the accumulation of moisture (as it will we shown next). The accumulation mode ceased abruptly during the passage of the perturbation on August 10: cyclone *Ilse*, located over the Gulf of Genoa at that day (not shown) inhibited the coastal convergence of sea-breezes and the subsidence over the western basin, and forced intense south-westerlies over the region. On the early morning of August 12 (Figure 1c), the cyclone reached its lowest pressure over Central Europe and started to leave the area, advancing fairly slowly eastwards. Normal (close-to-mean) conditions were completely restored after August 15 (Figure 1d). The target area, getting the highest precipitation amounts during the episode, was a vast region comprised between 45-

53°N latitude and 8-16°E longitude and it is marked with a square.

3 Setting up the high resolution simulations

Following a meaningful explanation of the episodes of long range transport of ozone in northern Iberia and the WMB (Gangoiti et al., 2001, 2006b), and the mechanism for the accumulation and exportation of the Saharan soil dust and pollution from southern Europe to the tropical Atlantic and the Caribbean (Gangoiti et al., 2006a), we were encouraged to use a similar modelling system to explore the preferred pathways, time(s) of travel, as well as convergence and venting mechanisms for the exportation of these accumulation layers.
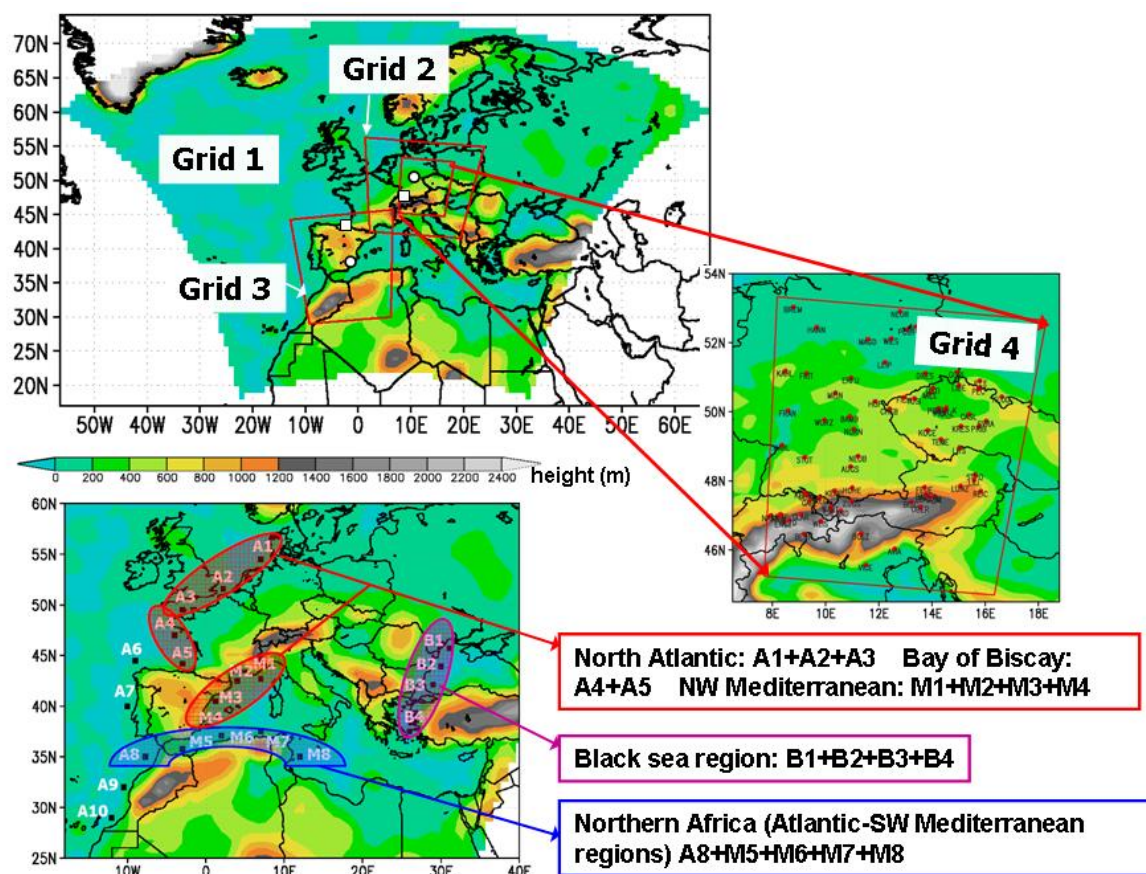
Figure 2. Topography and coverage of domains for the RAMS-HYPACT modelling system. The location of the wind profiler radars and the selected sounding sites, shown in Figures 3 and 4, has been represented by closed white squares and circles, respectively. Grid 4 (right) is approximately coincident with the target area of precipitation. The position of the HYPACT tracer sources are represented at the lower-left panel.

Latest versions of Regional Atmospheric Modelling System (RAMS) and HYbrid PArticle Concentration and Transport model (HYPACT) modelling systems are applied here. RAMS (Pielke et al., 1992) is a nonhydrostatic model with a highly versatile numerical code; HYPACT (Tremback et al., 1993) is a combination of a Lagrangian particle model and Eulerian concentration transport model.

The domain coverage and resolutions used in prior simulations have been modified aiming to adequately simulate the transport of vapour from the source areas into the precipitation target area (Figure 2). Four nested grids are used for the simulation: the finest grid (4) is approximately coincident with the target area of precipitation and it has a resolution of 9 km, intermediate grids 2 and 3 have a resolution of 27 km, and, the lowest resolution (108 km) corresponds to grid 1, including Europe, the whole Mediterranean and part of the Atlantic Ocean. Two-way nesting is allowed between the grids, so that the higher-resolution grid conditions the flow in the lower-resolution grid and vice versa. Four-dimensional data assimilation was used for the model run, with Newtonian relaxation towards the 6-hourly

NCEP Reanalysis daily data during the whole simulation (Kanamitsu et al., 2002): a variable relaxation time was used, with the highest values (weak nudging) at the center of the large domain (grid 1) and lowest values (strong nudging) at the boundaries. Since the precipitation in central Europe was significantly above average in the weeks before the studied episode, we decided to start the simulation on July 27 and run it continuously through August 16, 2002. Starting the simulation two weeks before the analyzed episode allows us to capture more accurately the soil moisture availability. The topography and land cover were interpolated from the USGS global 30" lat-long database (Gesch et al., 1999; Anderson et al., 1976). Weekly averages of the sea surface temperature (SST) data, with a $1° \times 1°$ resolution, were interpolated from the NCEP Reynolds SST dataset (Reynolds and Smith, 1994) during the model run. Our setup included a prognostic turbulent kinetic energy (level 2.5) parameterization (Mellor and Yamada, 1982), with modifications for a case of growing turbulence (Helfand and Labraga, 1988), and a full-column two-stream parameterization that accounts for each form of condensate (7 species) for the calculations of the radiative
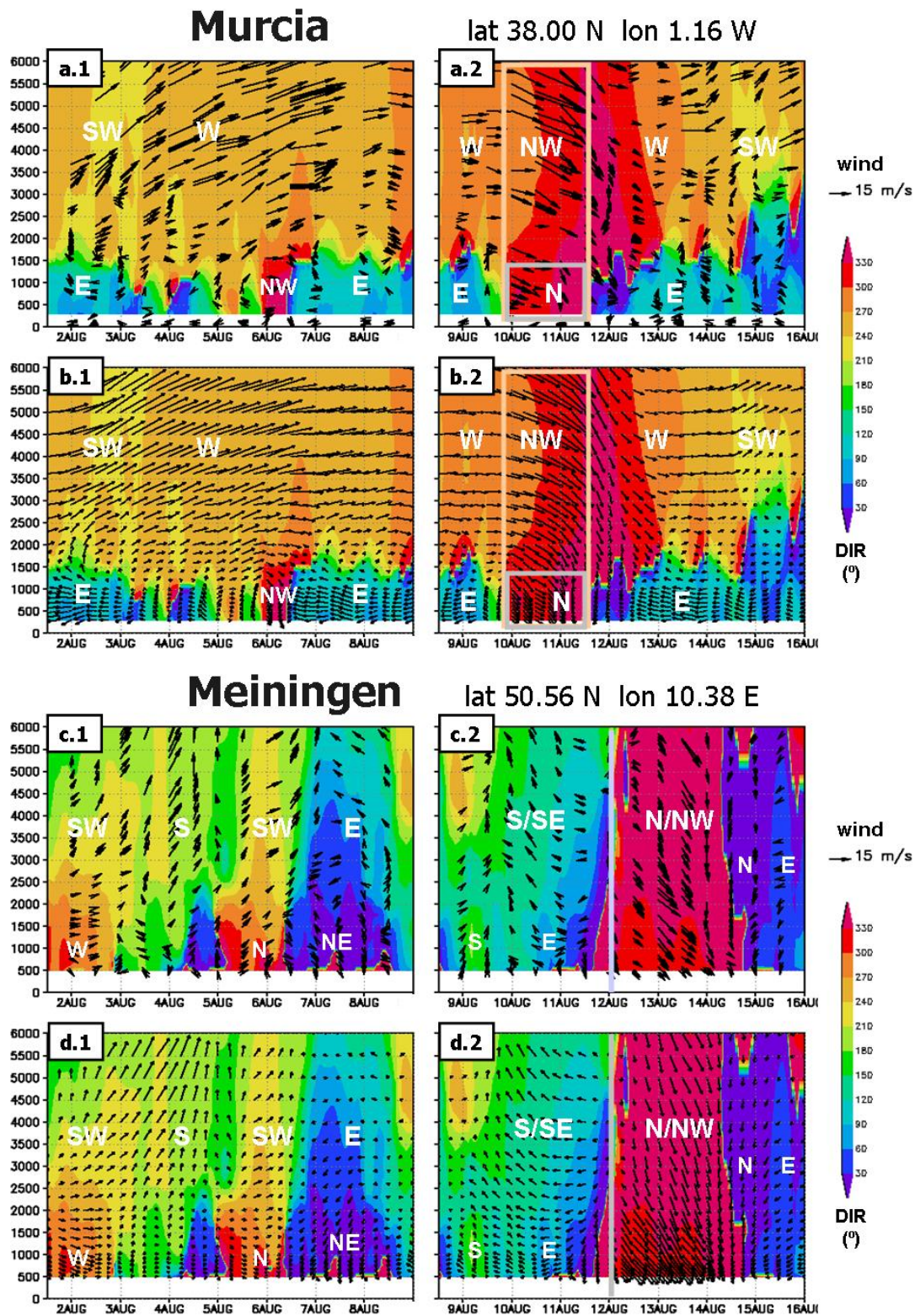
Figure 3. Sequence of radio-sounding wind profiles observed at Murcia from August 2 to 16 (a.1, a.2) and Meiningen (c.1, c.2), together with simulated winds profiles estimated by RAMS at the same locations: Murcia (b.1, b.2) and Meiningen (d.1, d.2). Shaded colours (all panels) represent the wind direction estimated by the mesoscale model. The suppression of the mesoscale processes when *Ilse* irrupted into the Western Mediterranean basin (the area inside the grey box, a.2 and b.2) as well as the change in the origin of the air masses arriving to Meiningen on August 12 (marked by solid grey line, c.2 and d.2) are well estimated.

transfer (Harrington et al., 1999). The cloud and precipitation scheme by (Walko et al., 1995) was applied in all domains with all species activated, and the soil vegetation scheme LEAF-3 was used to calculate sensible and latent heat fluxes exchanges with the atmosphere (Walko et al., 2000).

Hourly meteorological fields given by RAMS were fed to the HYPACT model to track the water vapour from a selection of sources. Figure 2 illustrates the position of the tracer sources, comprising a total of 22 vertical emission lines, from surface level to 500 m height. They are placed at the main entrances of marine water vapour to continental areas: WMB, the Atlantic Ocean and the Black Sea coasts. The 5 shaded regions are used to show their respective contribution as 'area sources' by adding the tracer particles emitted from them to the target area. Particle release started 6 hours after the meteorological model initial time of simulation (06 UTC July 27) and lasted until August 14, while particle positions were tracked for the whole period of simulation (20 days). The emission, a total of 85200 particles per source, was continuous and constant. It should be stressed that HYPACT simulates the motion of atmospheric passive tracers, thus, emitted particles do not undergo chemical transformations or any type of removal mechanisms. It is evident, considering the lifetime of water vapour in troposphere, that after 8-10 days of transport, around half of the initial water vapour contained in the tracked air mass will probably be removed and replaced by rainfall and evaporation during the trajectory, while our particles still remain the same. We have assumed, thus, that trajectories with short transit times (less than 8-10 days) ending in the target area of precipitation, and especially after travelling through the boundary layer of warmer wet lands and water bodies, will be associated with the vapour originating the precipitation event, although we assume the actual occurrence of evaporation/precipitation en route. To the contrary, larger transit times and/or air mass trajectories away from the target during the rainfall period will show their null or minor contribution.

4 Results and discussion

Two different types of results are discussed here: Section 4.1 is devoted to the discussion of mesoscale modelling results and their comparison with experimental data, and Section 4.2 concentrates on the examination of the contribution of the main potential source areas of water vapour to the Elbe/Danube flood.

4.1 Experimental data and mesoscale modelling results

To determine whether the selected setup of the modelling system was able to reproduce the main meteorological fields at different scales and find an adequate configuration for this study, we tested several options changing the

number of grids, the domain coverage, the resolution and the nudging scheme. At every trial, we validated the RAMS meteorological output with NCEP data, wind and temperature profiles of the European NMC stations, output from Wind Profiler Radars (WPR) at Bilbao (Spain) and Basel (Switzerland), surface precipitation at the target area, MODIS total precipitable water vapour and precipitation data from the TRMM Multi-Satellite Precipitation Analysis (TMPA). Results shown here were found to be the best representation of the mentioned set of observations.

Hourly wind speed and direction calculated by the model and the experimental measurements of two rawinsonde soundings and two WPRs during the same period are represented in Figures 3 and 4. Their location is shown in Figure 2. It can be checked that simulated and observed wind profiles agree satisfactorily: the high resolution simulation was able to capture both the intensity and the timing of the coastal sea-breezes and drainage winds registered in Murcia (Spain) under weak synoptic conditions, and the suppression of these mesoscale flow regimens coincident with the passage of *Ilse* on August 10-11 (marked with a grey square, a.2 and b.2), as well as the transition from southerly to north-westerly winds registered in Meiningen (Germany) on August 12 (indicated with a grey line, c.2 and d.2). The same can be concluded from the comparison of the modelled wind profiles with Bilbao's and Basel's WPRs outputs (Figure 4), as they appear to be consistent with our simulation. The statistical values (BIAS, RMSVE, RMSE and correlation, defined by Zhong and Fast, 2003), summarized in Table 1, confirm the visual impression arising from the previous figure: despite a slight general underestimation, our RAMS set-up was capable of simulating wind profiles with statistical scores comparable to those of other similar studies (Hanna and Yang, 2001; Carvalho et al., 2002; Zhong and Fast, 2003).

Figure 5 illustrates the 72-hour accumulated precipitation during the episode (August 10-13). The distribution of simulated precipitation (left panel) and the surface station data depicted by Rudolf and Rapp (2003) (right) cover a similar region and the mesoscale model has also reproduced the general distribution and amount of precipitation. Figure 5, as well as the TMPA data (Figure 6), shows that wide areas around Germany's border with the Czech Republic and Austria experienced rainfall totals above 180 mm in 2 days. Conversely, out of the target region, with lower grid-cell resolutions, the simulated amounts are considerably smaller than the TMPA observations.

The water vapour total column is represented in Figure 7 for August 9 to 12, as shown by MODIS-TERRA IR images (left panels) and RAMS model simulations (right panels). The upper panels show the end of the accumulation mode in the WMB while the lower three ones illustrate the subsequent venting of the vapour over the Mediterranean, ahead of the perturbation. The mesoscale atmospheric circulations, mentioned in section 1, accumulated in 4 days (from August 6 to August 9) over 4.0 cm of water vapour over the area between
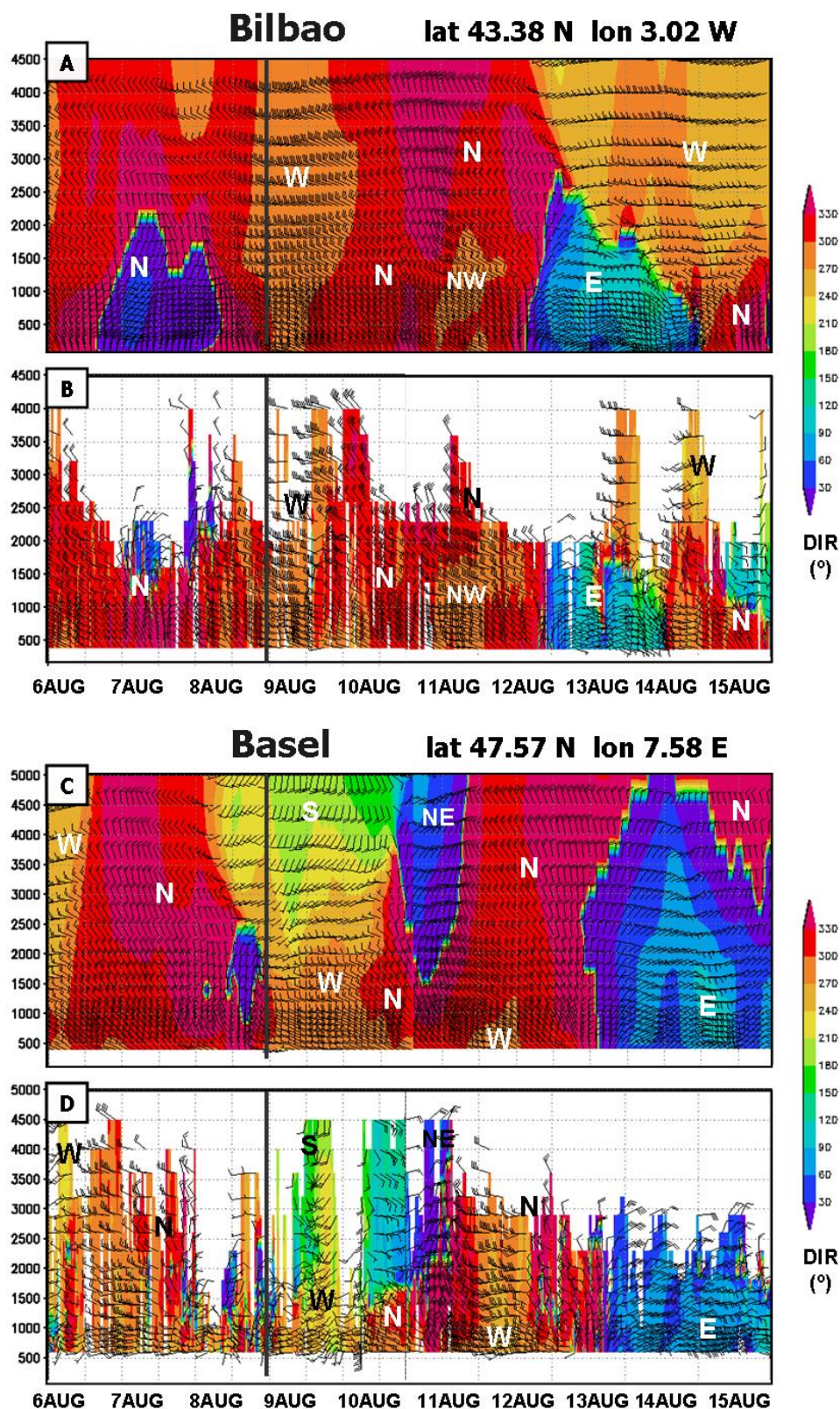
Figure 4. (Top) Time sequence of the observed (a, c) and simulated (b, d) wind profiles on the vertical of two wind profiler sites, Bilbao (top) and Basel (bottom), from August 6 to 16. The wind direction is depicted in shaded colours. RAMS has adequately reproduced the change that the passage of the cyclone provoked in these sites (marked by solid black lines).
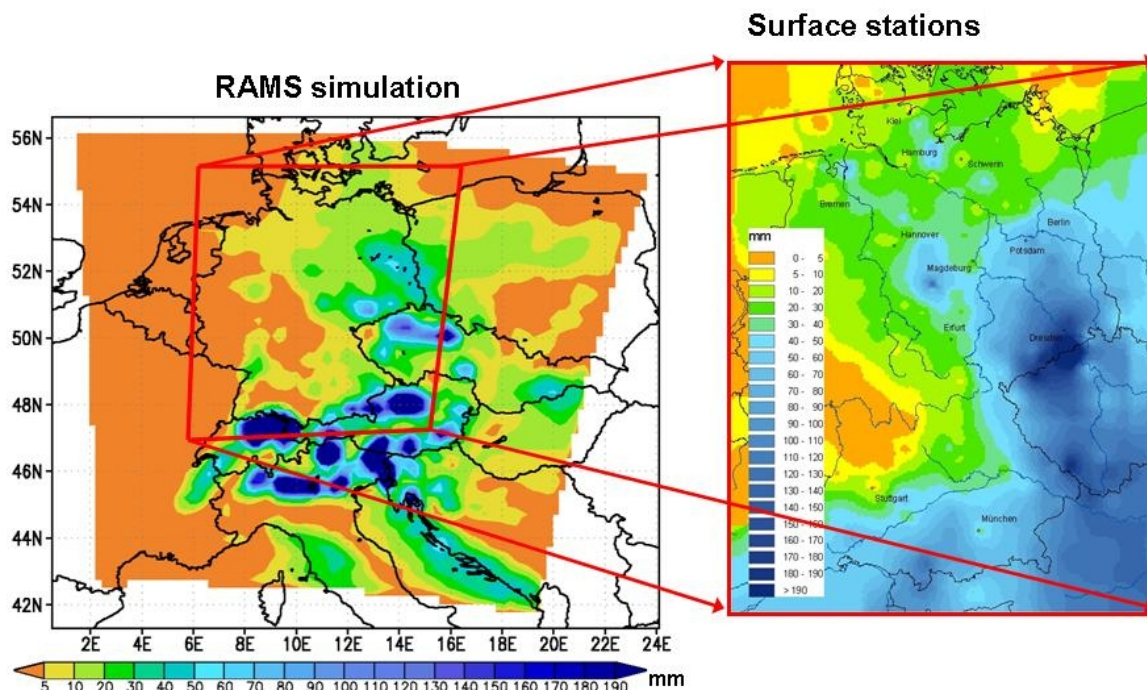
Figure 5. Distribution of simulated precipitation (left panel) and interpolated surface station data (right, courtesy by B. Rudolf, GPCC and Deutscher Wetterdienst), as depicted by Rudolf and Rapp (2003): totals from 06 UTC August 10 to 06 UTC August 13. Precipitation maxima, in both figures, are distributed at the southern and eastern corners of a vast region, including Switzerland, western Austria, western Czech Republic and some regions in south and east Germany.

the East coast of Iberia, northern Africa and the Balearic Islands. On August 10, this large water vapour column was advected towards the E and NE and it is observed as a cyclonically curved band throughout central Europe on August 11 and eastern Europe on August 12. Apart from the differences in the lower left corner of the figures, where vapour from the African Inter Tropical Convergence Zone outbreaks into the Atlantic, the simulated and observed water vapour column agree satisfactorily during the whole simulation period, confirming that the water vapour transport associated with the rainfall episode was well captured by the simulation.

Figure 8 (left panels) depicts the water vapour column between the 700-300 hPa pressure levels observed by MODIS as well as the simulated wind fields at 3600 m MSL on August 6, 9 and 10. The comparison of these columns with the water vapour columns between the surface and the 700 hPa pressure level (middle panels) reveals that practically all the vapour over N-Africa, above latitude 25°N, is at that height range (700-300 hPa). This anomalous vertical distribution, with the lowest values at the surface and increasing with height to reach maximum values at the middle troposphere, results from the same meteorological mechanism responsible for the accumulation of dust around the Atlas Mountains; for this case, it applies to the conver-

gence and recirculation of water vapour vented to the middle troposphere by the combined orographic upslope flows and Mediterranean and Atlantic coastal sea-breezes around the Atlas Mountains. The panels on the right, an enlarged view of the WMB, allow us to show the changes in the distribution of water vapour column and the wind fields during normal and perturbed conditions. From August 6 to August 9, a period that corresponds to the initiation and to the ending of the accumulation mode, the coastal convergence (sea breezes-upslope flows) and sinking over the WMB accumulated vapour over the reservoir layers of the basin, following the aforementioned scheme by Millán et al. (1997), while convergence around the Atlas Mountains fed the middle troposphere reservoir over northern Africa. The mechanisms behind this accumulation are illustrated in the vertical cross sections of the simulated water vapour mixing ratio (shaded colours) and the cross wind components (u-w and v-w streamlines) at a constant latitude 38°N (Figure 9, a.1 and b.1) and at a constant longitude 0° (Figure 9, a.2 and b.2) during these two days (August 6 and 9, 12 UTC). Panels a.1 and a.2 show the deep vertical injections that take place both over eastern Iberia (3000 m) and over northern Africa (>5000 m). These injections and their return flows lead to the vertical recirculation of the water vapour and to its accumulation over the WMB (panels b.1
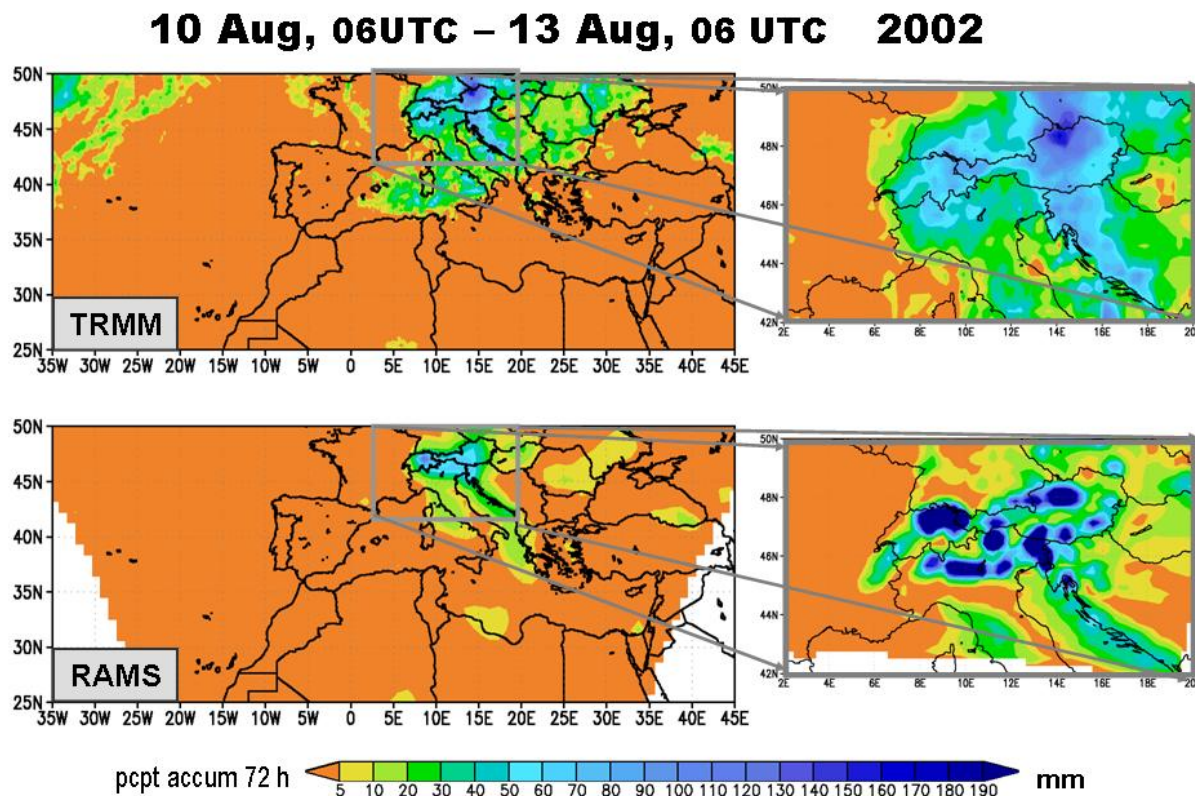
Figure 6. Precipitation amounts over Southern Europe derived from TRMM Multi-Satellite Precipitation Analysis data (top) and simulation output (bottom), from 06 UTC August 10 to 06 UTC August 13. Right panels zoom into the target area.

and b.2), whereas another fraction is transported within the anticyclonic gyre of the N-African mid-tropospheric circulation. The layer containing more than 4 g kg^{-1} of water vapour extends up to 3000-4000 m over eastern Iberia and northern Africa on August 9. Significant differences can be observed on August 10 (Figure 8, c.3) that shows the effects of the passage of the Atlantic cyclone *Ilse* over the WMB: the sea-breeze convergence over the crest of the mountains is inhibited, and the frontal system forces intense southwesterlies over the area venting off the water vapour into central and eastern Europe, reducing the total column of water vapour over the WMB from 3.75-4.0 to 1.75 cm in less than 12 hours: Figure 10, discussed in the next section devoted to the tracing experiments, also shows the venting of the WMB.

These results show the ability of the mesoscale model to reproduce the details of the flows within the region of interest as well as to explain the distribution of the water vapour, its layering, and transport with a sufficiently good level of accuracy. Two questions have to be addressed now: (i) the source of the vapour responsible for the central Europe precipitation events on August 11-13, and (ii) the role of the WMB and N-African vapour accumulation layers in the precipitation of the target area.

4.2 Simulated water vapour accumulation and transport processes

In order to determine where the water that resulted in extreme rainfalls on August 11-13 evaporated, the trajectories of passive tracers flowing out the main marine sources of water vapour into continental areas were examined.

Figures 10 and 11 present the track of the tracer released from the N-Atlantic region (left panels) and the age or the travel time of the tracked particles (right panels) on August 9 and 10 (Figure 10) and 11 to 13 (Figure 11). Arrows show the wind transporting the main fraction of the tracer. On August 9, the accumulation period over the WMB, initiated on August 6 after a massive intrusion of an air mass of a N-Atlantic origin, entered on its last day. On the upper-left panel they show the main paths into the Mediterranean (southern France and the Gulf of Lyon) and once inside the basin, the western branch follows the combined upslope flows and coastal sea-breezes of eastern and northern Iberia, while the eastern branch drifts slowly southwards, parallel to the Italian Peninsula. According to our simulations (not shown in the Figures), the major fraction of the tracer was transported over the Mediterranean Sea at the lower troposphere (0-2000 m). For the lower 1000 m, RAMS estimates that the water vapour entered the Mediterranean with an average mixing ratio of
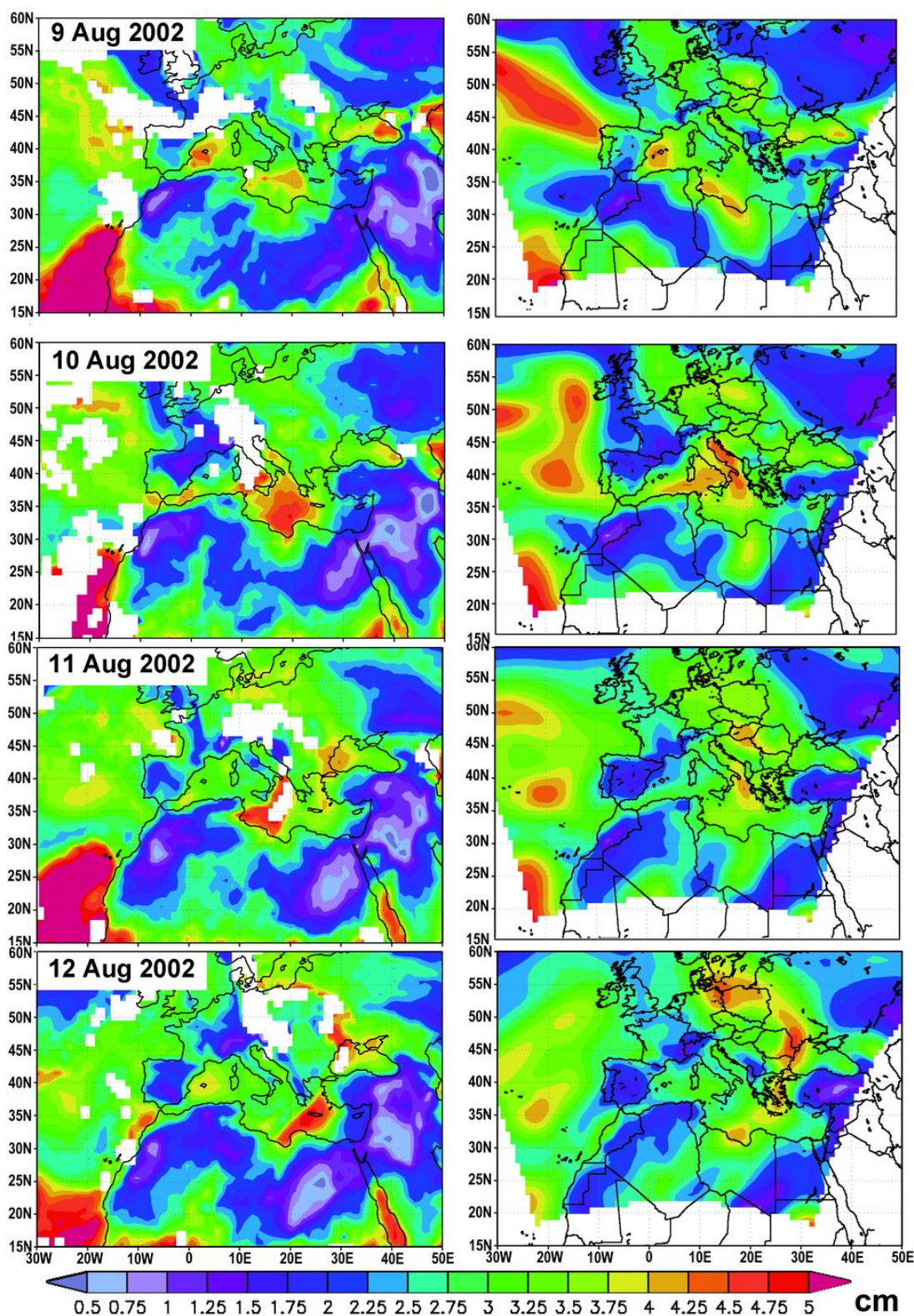
Figure 7. Water vapour total column, as shown by MODIS-TERRA IR images (left panels) and by the model RAMS simulations at the time of the satellite's overpass (right panels), from the end of the accumulation mode on August 9 to August 12: the water vapour positive anomaly in the Western Mediterranean basin (August 9) is swept by the frontal passage on August 10. Two days after (August 12), there is again evidence of a new vapour accumulation in the Western Mediterranean basin. In the MODIS panels areas covered by clouds (in white colour) contain no vapour data.
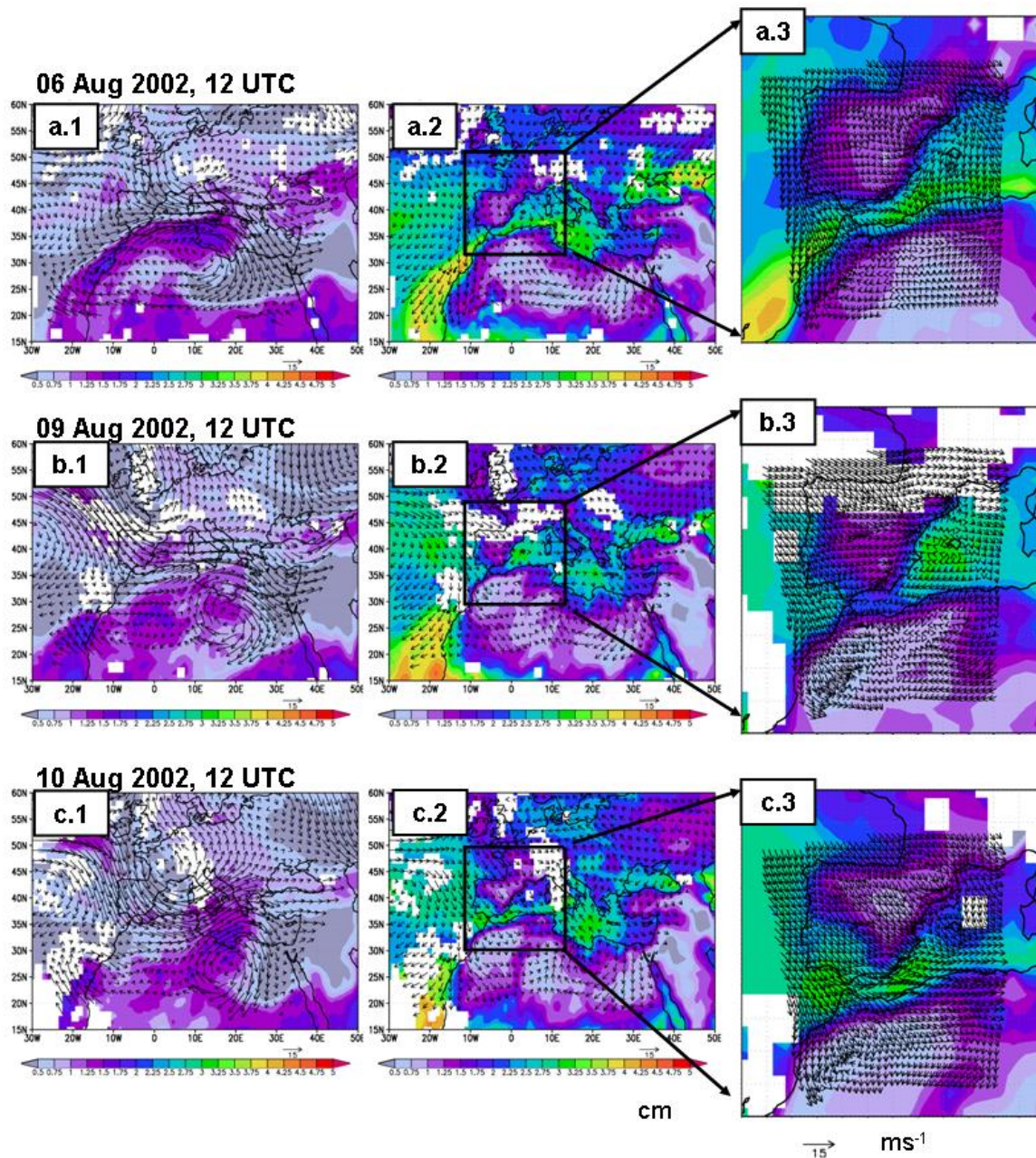
Figure 8. (Left) MODIS water vapour column between 700-300 hPa, together with simulated winds (grid 1) transporting the vapour (winds at 3600 m above ground). (Middle) MODIS water vapour column from ground level up to 700 hPa together with winds at ground level.(Right) Enlarged view of the MODIS lower water column, together with surface wind simulations at grid 3 on August 6, 9 and 10.

8.5 g kg^{-1} and exited with 12.5 g kg^{-1}, after being transported through Italy and the Adriatic Sea. Then, it crossed the Western Balkans and Eastern Europe into the target area during August 10 (lower panels): red arrows indicate that the N-Atlantic tracer was vented to the middle and upper troposphere. The low level flow forced by the Scandinavian Anticyclone, behind the perturbation, is marked with a white arrow.

Similar tracks are seen for the tracer emitted from the Bay of Biscay and from the WMB itself (not shown). The massive intrusion into the WMB for the tracer released at the Bay of Biscay also occurred on August 6 through the Gulf of Lyon. A smaller fraction crossed Iberia over the Ebro Valley into the WMB. Main differences with the N-Atlantic tracer are related with the time of arrival to the target area on August 11. As mentioned in the previous paragraph, the main fraction of the joint tracer released from all these
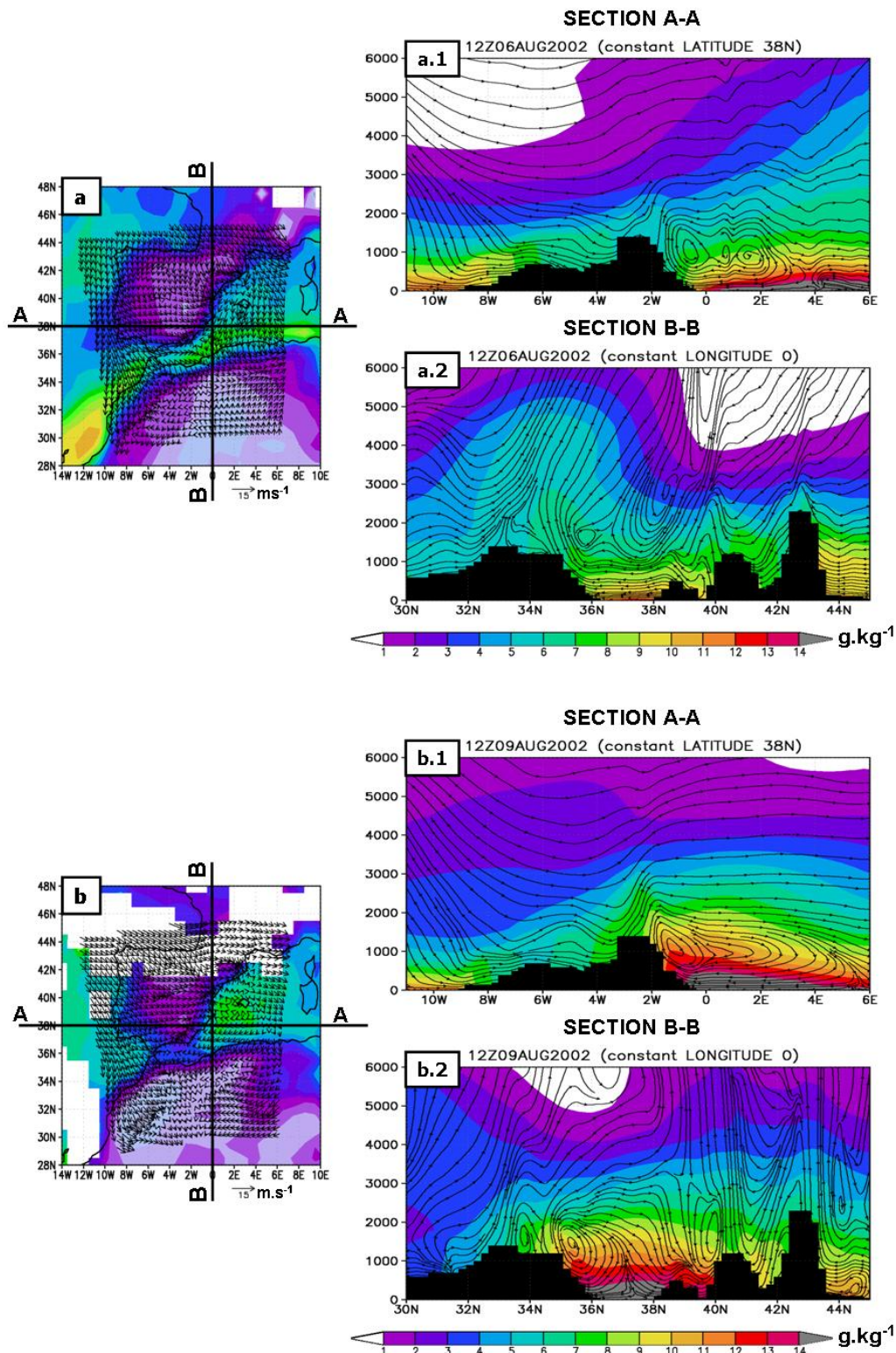
Figure 9. Sequence of the vertical distribution of the simulated vapour mixing ratio during a full period of accumulation (6-9 August) in the Western Mediterranean basin. MODIS water vapour shown in a and b depict the position of the cross sections deployed on the right: panels a.1 and b.1 show vertical cross sections, centered at constant latitude $38°$N, of water vapour and simulated u-w streamlines; while a.2 and b.2 are centered at constant longitude $0°$, and show water vapour with v-w streamlines. The terrain factor scale (horizontal-to-vertical ratio in the cross-sections) has been considered for streamlining to favour the interpretation. Terrain profile is represented (in black) at the bottom.
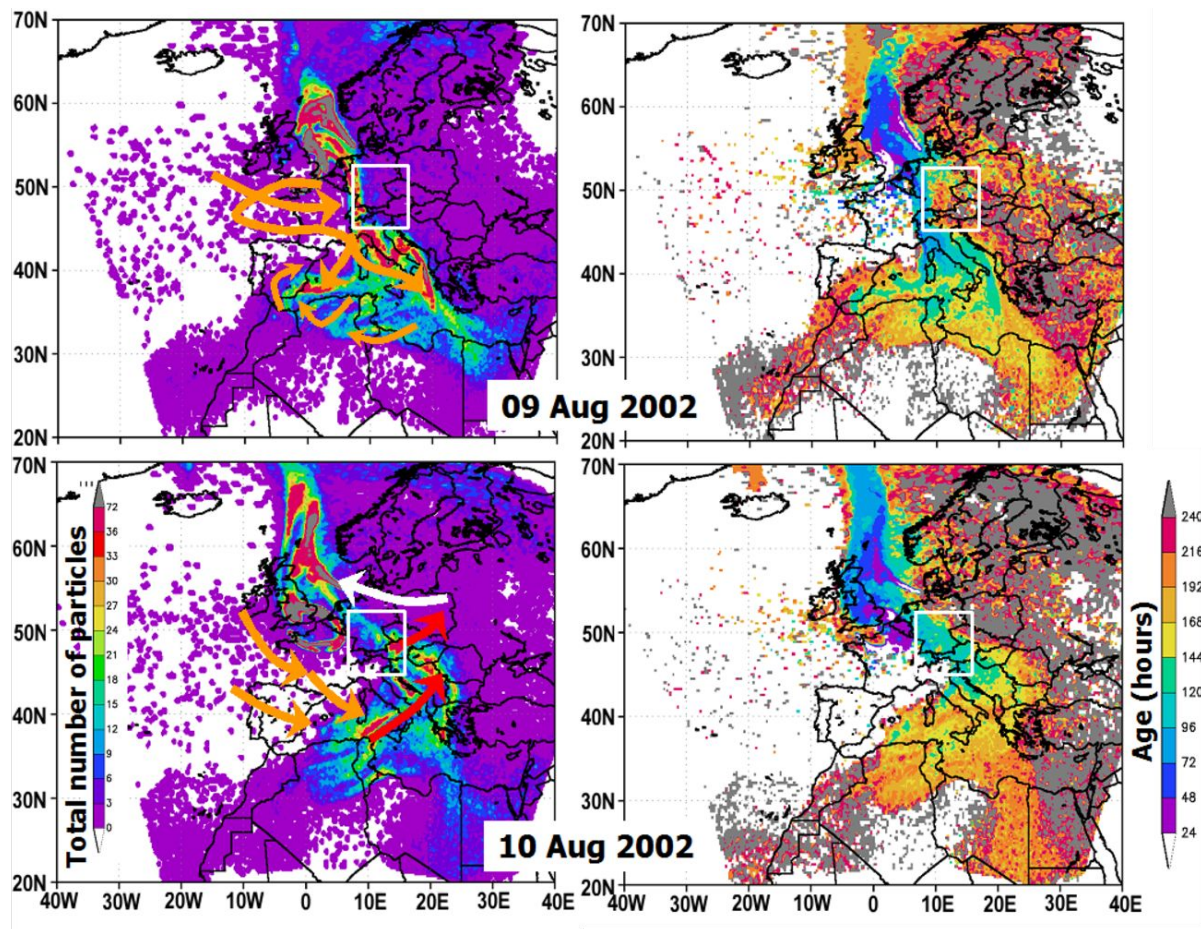
Figure 10. Tracks of the N-Atlantic tracer (total number of particles) at the end of the accumulation period of the Western Mediterranean basin on August 9 (upper left) and after the irruption of the perturbation caused by cyclone *Ilse* (lower left), and age of the respective tracks (right panels). The perturbation vented the accumulated vapour out into the target area (white square): red arrows at the lower-left panel indicate that the tracer is vented to the middle and upper troposphere, ahead of the frontal system.

sources (marked in red in Figure 2) was vented to the middle and upper troposphere (0-8000 m) before arriving at the latitudes of the target area. These joint air masses, could have entrained additional water from evapotranspiration over the Western Balkans before arriving to the target area on August 11. Model results, however, show that precipitation during the trajectory over the Balkans would have probably compensated the evapotranspiration, since the water vapour total column remained constant within the air mass (4 cm), and the average vapour mixing ratio of the lower 1000 m kept at the same values as when leaving the Adriatic Sea (12.5 g kg^{-1}).

Figure 11 (upper-left panel) shows the N-Atlantic tracer's path to the target area on August 11. After crossing the Western Balkans and Eastern Europe, it veered to the West pointing to the low pressure region developed at the northern flanks of the Alps during the evolution of the cyclone *Ilse*. The age of the tracer this day is 168 hours, that is, it was emitted on August 4 from the N-Atlantic region and, after a long journey across the WMB, moved to the North again. The tracer reached the latitudes of the target area not

so far from the region where it was released 7 days before, at that time flowing within a colder and drier air mass. On August 11, while the tracer moved slowly to the West, parallel to the northern flanks of the Alps, intense precipitations were registered over the target region, and the pressure decreased to their minimum values. The lowest two panels in Figure 11 show how on August 12 and 13 cool N-Atlantic air moved across northern France, in a direct NW-to-SE trajectory towards the target area, facing and replacing the old, humid, and warmer air-mass located over the region. The frontal system formed by the two air masses is better observed in the right panels, looking at the age of the tracer over the target area: blue colours face the more reddish colours of the old tracer. Intense precipitations were also registered at the region during August 12 until the early morning of August 13: rainfall events moved into the E and NE region of the target area, following the slow movement of the frontal system.

From August 12 at 12 UTC until August 13 at 12 UTC intense rain episodes were also registered in the western
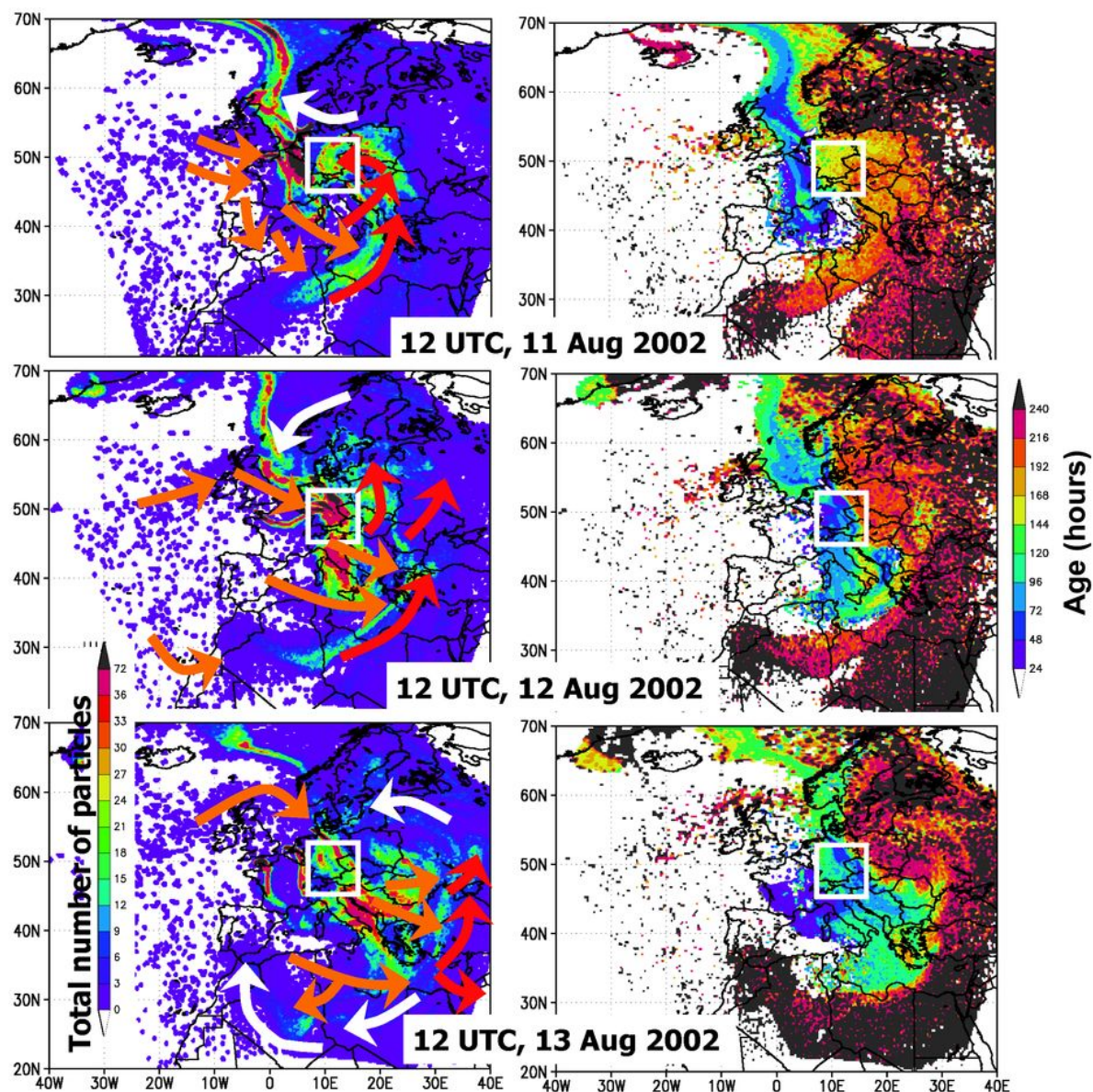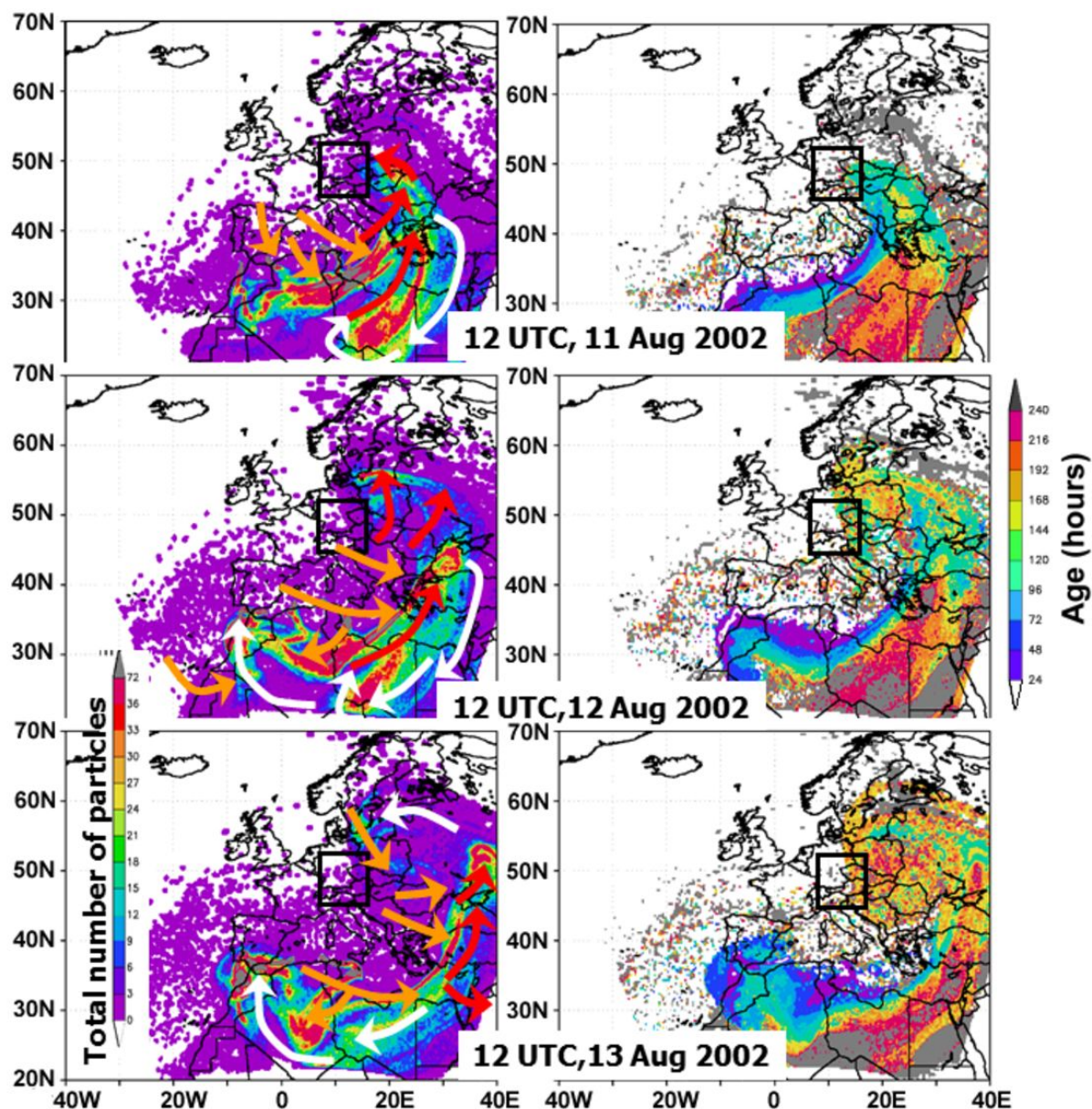
Figure 11. Tracks of the N-Atlantic tracer during the rainfall maxima in central Europe from August 11 to 13 (left), and age of the tracks (right). The tracer crossing the Western Balkans on 10 August, moved westward into the target area of central Europe on 11 August (upper left). This aged tracer (right panels) faced new tracer emissions with the same N-Atlantic origin travelling directly inland into the target region on August 12 (middle panels). At the same time, over southern Europe, the perturbation crossed the central Mediterranean. During the morning of August 13, the old tracer was removed from central Europe (lower right), the precipitation decreased at the region, and intensified at the Black Sea.

Black Sea region (Bulgaria, Romania and Ukraine), moving from the SW to the NE of the region, ahead of the frontal system located over the Mediterranean Sea and associated with cyclone *Ilse*. However, the origin of the water vapour contained in the air mass running ahead of the frontal system at the Black Sea has to be defined, and will be discussed in the following paragraphs.

To explore the role of the N-African accumulation layers, we tracked the trajectories of the tracer emitted from the

blue coloured area in Figure 2. As displayed in Figure 12, it did not penetrate deep into the target area of central Europe and moved around the East and North boundaries of this region. In spite of this, during the severe rainfalls registered in the Western Black Sea region (August 12-13), the N-African tracer can be observed running ahead of the frontal system, which entered the eastern Mediterranean on August 12. The tracer, accumulated in the middle troposphere, was vented out with the south-westerlies over the Western region of the

Figure 12. Tracks of the N-African tracer during the rainfall maxima in central Europe from August 11 to 13 (left), and age of the tracks (right). The main fraction of the N-African accumulation layers, following the tracer trajectories (red arrows), did not penetrate into the target area of central Europe, now marked with a black square. However, during the second half of August 12 and during August 13, intense rainfalls were registered in wide areas of the western Black Sea region. At the time of the rainfall events, the N-African tracer travelled ahead of the frontal system, entering the eastern Mediterranean on August 13.

Black Sea. The lower two rows of panels in Figure 12 show the recovery of the accumulation mode of the middle troposphere of N-Africa, initiated by the restitution of the upper flow behind the frontal system (white arrows) as described by Gangoiti et al. (2006a).

The distribution of the tracer released from the violet coloured region in Figure 2 reveals that these potential sources of water vapour did not contribute to the precipitation in central Europe during the first stage of the episode (not shown). On August 12, this tracer is found, together

with the N-African one, over the area of Bulgaria, Romania, and Ukraine, ahead of the frontal system crossing the Mediterranean. The joint plume occupies a large band which crosses the Aegean Sea, the western Black-Sea, and to the NW over Poland into the Baltic Sea. This location is equal to the position of the water vapour front shown both in the MODIS data and in the mesoscale model simulations (Figure 7, lower panels). Nonetheless, during the final stage of the event, the tracers, emitted 3-4 days before from the NW region of the Black Sea, moved into the north-eastern border

of the target area, suggesting that evaporation from this region could have fed the rainfall on August 13.

There is a general agreement between the findings presented here and the relative contribution of the different source areas quantified applying a new Lagrangian backward trajectories method, developed by our group in the UPV-EHU and *Fundación Centro de Estudios Ambientales del Mediterráneo*. The results of this innovative approach, inspired in the pioneering work by Dirmeyer and Brubaker (1999), show that the most important fraction of the attributed evaporation that caused the extreme rainfalls of August 11-13 took place between 6 to 8 days before the precipitation event and that the distribution of evaporative sources changed from day to day along the rainfall episode (Gangoiti et al., 2011). The evaporation sequence corroborates the role and the importance of the WMB accumulation mechanism in the first part of the torrential rainfall episode (from August 11 until August 12 at 12 UTC) as well as the significant contribution of evaporation from northern and eastern land areas in its second part (from August 12 until the early morning of August 13).

5   Conclusions

In this paper we presented the results obtained in the analysis of experimental data and high resolution simulations of one of the most severe precipitation events experienced in Central Europe (August 11-13, 2002). Our results show that water vapour from different sources contributed to the extreme precipitation event at different periods of time.

According to our results, during the first stage of the episode most of the precipitation came from an air mass exported from the WMB. That air mass, with an initial Atlantic origin, entered the Mediterranean on August 6, mainly through the Gulf of Lyon and split into two branches. The western branch circulated within the MBL and the coastal range of mountains of western Iberia and northern Africa, accumulating vapour in reservoir layers on top, by the combined upslope flows and sea-breezes. Another branch of that air mass followed a N to S trajectory parallel to the Italian Peninsula evaporating water vapour from the Ligurian, Tyrrhenian and Adriatic Seas. On August 10, most of that water vapour was transported after the irruption of the *Ilse* cyclone, throughout Italy and the Adriatic Sea, across the Western Balkans into the target area initiating the rainfall episode on August 11. Evapotranspiration en route on the landmass, before arriving at the target region, could have contributed to compensate the precipitation losses while crossing the Western Balkans during the initiation of the episode. During August 12 there was a transition in the origin of air masses arriving to the target region from the western Mediterranean to the Atlantic. Those colder air masses irrupted in a direct NW-to-SE direction into the low pressure area developed at the target region pushing the Mediterranean air mass out of the area. The frontal system formed by the two air masses moved slowly across the target region to

the East, and caused intense precipitations until the morning of August 13. Additionally, on August 12 and 13, evapotranspiration during the trajectory over the south-eastern European land mass, could have played a non-negligible role increasing the available humidity for precipitation because of the presence of a moist land surface after the previous cyclone circulation over the area on August 6-7.

Other marine sources of water vapour, like those feeding the accumulation layers in the N-African middle troposphere and over the Black Sea region, seem not to have an important contribution to the rainfall in central Europe. They could, however, be connected with the intense events observed in Bulgaria, Romania and Ukraine during the second half of August 12 and 13.

References

Anderson, J. R., Hardy, E. E., Roach, J. T., and Witmer, R. E., 1976: A land use and land cover classification system for use with remote sensor data, U.S. Geological Survey Professional Paper, Government Printing Office, Washington D.C., 964, 28 p.

Carvalho, J. C., Anfossi, D., Trini Castelli, S., and Degrazia, G. A., 2002: *Application of a model system for the study of transport and diffusion in complex terrain to the TRACT experiment*, Atmos Environ, **36**, 1147–1161.

Christensen, J. H. and Christensen, O., 2003: *Severe summertime flooding in Europe*, Nature, **421**, 805–806.

Dirmeyer, P. A. and Brubaker, K. L., 1999: *Contrasting evaporative moisture sources during the drought of 1988 and the flood of 1993*, J Geophys Res, **104**, 19 383–19 397.

Fricke, W. and Kaminski, U., 2002: *Ist die Zunahme von Starkniederschläen auf veränderte Wetterlagen zurückzuführen?*, GAW Brief des Dtsch Wetterdienstes, **12**, 1–2.

Gangoiti, G., Millán, M. M., Salvador, R., and Mantilla, E., 2001: *Long-range transport and re-circulation of pollutants in the Western Mediterranean during the RECAPMA Project*, Atmos Environ, **35**, 6267–6276.

Gangoiti, G., Alonso, L., Navazo, M., García, J. A., and Millán, M. M., 2006a: *North African soil dust and European pollution transport to America during the warm season: hidden links shown by a passive tracer simulation*, J Geophys Res, **111**, D10 109, doi: 10.1029/2005JD005 941.

Gangoiti, G., Albizuri, A., Alonso, L., Navazo, M., Matabuena, M., Valdenebro, V., García, J. A., and Millán, M. M., 2006b: *Sub-continental transport mechanisms and pathways during two*

ozone episodes in northern Spain, Atmos Chem Phys, **6**, 1469–1484.

Gangoiti, G., Gomez-Domenech, I., Sáez de Cámara, E., Alonso, L., Navazo, M., Iza, J., García, J. A., Ilardia, J. L., and Millán, M. M., 2011: *Origin of the water vapor responsible for the European extreme rainfalls of August 2002: 2. A new methodology to evaluate evaporative moisture sources, applied to the August 11-13 Central European rainfall episode*, J Geophys Res, **116**, D21 103, doi: 10.1029/2010JD015 538.

Gesch, D. B., Verdin, K. L., and Greenlee, S. K., 1999: *New land surface digital elevation model covers the earth*, Eos, Transactions, American Geophysical Union, **80**, 69–70.

Hanna, S. R. and Yang, R., 2001: *Evaluations of Mesoscale Model's simulations of near surface winds, temperature gradients and mixing depths*, J Appl Meteorol, **40**, 1095–1104.

Harrington, J. Y., Reisin, T., Cotton, W. R., and Kreidenweis, S. M., 1999: *Cloud resolving simulations of Arctic stratus. Part II: Transition-season clouds*, Atmos Res, **51**, 45–75.

Helfand, H. M. and Labraga, J. C., 1988: *Design of a nonsingular level 2.5 second-order closure model for the prediction of atmospheric turbulence*, J Atmos Sci, **45**, 113–132.

James, P., Stohl, A., Spichtinger, N., Eckhardt, S., and Forster, C., 2004: *Climatological aspects of the extreme European rainfall of August 2002 and a trajectory method for estimating the associated evaporative source regions*, Nat Hazards Earth Sys Sci, **4**, 733–746.

Kanamitsu, M., Ebisuzaki, W., Woollen, J., Yang, S. K., Hnilo, J. J., Fiorino, M., and Potter, G. L., 2002: *NCEP-DOE AMIP-II Reanalysis (R-2)*, Bull Amer Meteor Soc, **83**, 1631–1643.

Mellor, G. L. and Yamada, T., 1982: *Development of a turbulence closure model for geophysical fluid problems*, Re Geophys Space Phys, **20**, 851–875.

Millán, M. M., Artiñano, B., Alonso, L., Castro, M., Fernández-Patier, R., and Goberna, J., 1992: Mesometeorological cycles of air pollution in the Iberian Peninsula, Air Pollution Research Report 44, Commission of the European Communities, Rue de la Loi, 200 B-1040 Brussels, Belgium, D.G. XII/E-1.

Millán, M. M., Salvador, R., Mantilla, E., and Artiñano, B., 1996: *Meteorology and photochemical air pollution in southern Europe: Experimental results from EC research projects*, Atmos Environ, **30**, 1909–1924.

Millán, M. M., Salvador, R., Mantilla, E., and Kallos, G., 1997: *Photo-oxidant dynamics in the Western Mediterranean in summer: Results from European research projects*, J Geophys Res, **102**, 8811–8823.

Millán, M. M., Estrela, M. J., Sanz, M. J., Mantilla, E., Martín, M., Pastor, F., Salvador, R., Vallejo, R., Alonso, L., Gangoiti, G., Ilardia, J. L., Navazo, M., Albizuri, A., Artiñano, B., Ciccioli, P., Kallos, G., Carvalho, R. A., Andrés, D., Hoff, A., Werhahn, J., Seufert, G., and Versino, B., 2005: *Climatic feedbacks and desertification: the Mediterranean model*, J Clim, **18**, 684–701.

Mudelsee, M., Börngen, M., Tetzlaff, G., and Grünewald, 2004: *Extreme floods in central Europe over the past 500 years: Role of cyclone pathway "Zugstrasse Vb"*, J Geophys Res, **109**, doi: 10.1029/2004JD005 034.

Pielke, R. A., Cotton, W. R., Walko, R. L., Tremback, C. J., Lyons, W. A., Grasso, D., Nicholls, M. E., Moran, M. D., Wesley, D. A., Lee, T. L., and Copeland, J. H., 1992: *A comprehensive meteorological modelling system - RAMS*, Meteorol Atmos Phys, **49**, 69–91.

Reynolds, R. W. and Smith, T. M., 1994: *Improved global sea surface temperature analyses using optimum interpolation*, J Clim, **7**, 929–948.

Rudolf, B. and Rapp, J., 2003: The Century Flood of the River Elbe in August 2002: Synoptic Weather Development and Climatological Aspects, Quarterly Report of the German NWP-System, No. 2, 1 December 2002 until 29 February 2003, Part 1, Deutscher Wetterdienst, Business Area Research and Development: 18-23.

Tremback, C. J., Lyons, W. A., Thorson, W. P., and Walko, R. L., 1993: An emergency response and local weather forecasting software system, Proceedings of the 20th ITM on Air Pollution and its Applications, New York, Plenum Press: 423-429.

Ulbrich, U., Brücher, T., Fink, A. H., Leckebusch, G. C., Krüger, A., and Pinto, J. G., 2003a: *The Central European Floods in August 2002, Part I: Rainfall periods and flood development*, Weather, **58**, 371–376.

Ulbrich, U., Brücher, T., Fink, A. H., Leckebusch, G. C., Krüger, A., and Pinto, J. G., 2003b: *The Central European Floods in August 2002, Part II: Synoptic causes and considerations with respect to climatic change*, Weather, **58**, 434–441.

Van Bebber, W. J., 1891: *Die Zugstraßen der barometrischen Minima nach den Bahnenkarten Deutscher Seewarte für den Zeitraum von 1875-1890*, Meteorol Z, **8**, 361–366.

Walko, R. L., Cotton, W. R., Meyers, M. P., and Harrington, J. Y., 1995: *New RAMS cloud microphysics parameterization. Part I: The single-moment scheme*, Atmos Res, **38**, 29–62.

Walko, R. L., Band, L. E., Baron, J., Kittel, T. G. F., Lammers, R., Lee, T. J., Ojima, D., Pielke, S. R. A., Taylor, C., Tague, C., Tremback, C. J., and Vidale, P. L., 2000: *Coupled atmospheric-biophysics-hydrology models for environmental modelling*, J Appl Meteor, **39**, 931–944.

Zhong, S. and Fast, J., 2003: *An Evaluation of the MM5, RAMS, and Meso-Eta Models at subkilometer resolution using VTMX field campaign data in the Salt Lake Valley*, Mon Weather Rev, **131**, 1301–1322.